MEMORANDUM REPORT BRL-MR-3957

BRL

MUZZLE BLAST FROM 105MM M735 ROUND

JOHN KIETZMAN
KEVIN S. FANSLER
WILLIAM G. THOMPSON

JANUARY 1992

U.S. ARMY LABORATORY COMMAND

BALLISTIC RESEARCH LABORATORY
ABERDEEN PROVING GROUND, MARYLAND

NOTICES

Destroy this report when it is no longer needed. DO NOT return it to the originator.

Additional copies of this report may be obtained from the National Technical Information Service, U.S. Department of Commerce, 5285 Port Royal Road, Springfield, VA 22161.

The findings of this report are not to be construed as an official Department of the Army position, unless so designated by other authorized documents.

The use of trade names or manufacturers' names in this report does not constitute indorsement of any commercial product.

REPORT DOCUMENTATION PAGE

Form Approved
OMB No. 0704-0188

1. AGENCY USE ONLY (Leave blank)	2. REPORT DATE	3. REPORT TYPE AND DATES COVERED
	January 1992	Final Aug 90 - Feb 91

4. TITLE AND SUBTITLE
MUZZLE BLAST FROM 105MM M735 ROUND

5. FUNDING NUMBERS
1L162618AH80

6. AUTHOR(S)
John Kietzman
Kevin S. Fansler
William G. Thompson

7. PERFORMING ORGANIZATION NAME(S) AND ADDRESS(ES)
U.S. Army Ballistic Research Laboratory
ATTN: SLCBR-LF-F
Aberdeen Proving Ground, MD 21005-5066

8. PERFORMING ORGANIZATION REPORT NUMBER

9. SPONSORING/MONITORING AGENCY NAME(S) AND ADDRESS(ES)
U.S. Army Ballistic Research Laboratory
ATTN: SLCBR-DD-T
Aberdeen Proving Ground, MD 21005-5066

10. SPONSORING/MONITORING AGENCY REPORT NUMBER
BRL-MR-3957

11. SUPPLEMENTARY NOTES
Supersedes IMR 959, dated March 1991

12a. DISTRIBUTION/AVAILABILITY STATEMENT
Approved for public release
Distribution unlimited

12b. DISTRIBUTION CODE

13. ABSTRACT *(Maximum 200 words)*

The overpressure field around an M68 tank cannon firing an M735 round was studied. Pressure transducers were located from 15 to 400 calibers from the muzzle and at 30 degree increments around the gun. The investigation yielded a detailed picture of the flow field, as displayed by overpressure traces. Comparisons of the overpressure data with a prediction method show better agreement for the measured points nearer to the muzzle. The peak overpressure, time-of-arrival, and positive-phase-duration data will be used together with other gun blast data to modify and improve the present prediction method. Observed anomalous pulses were also investigated but their origins remain unknown.

14. SUBJECT TERMS		15. NUMBER OF PAGES
Fluid Dynamics	Impulse Noise	26
Muzzle Blast	Noise Measurements	16. PRICE CODE

17. SECURITY CLASSIFICATION OF REPORT	18. SECURITY CLASSIFICATION OF THIS PAGE	19. SECURITY CLASSIFICATION OF ABSTRACT	20. LIMITATION OF ABSTRACT
UNCLASSIFIED	UNCLASSIFIED	UNCLASSIFIED	Same as Report

INTENTIONALLY LEFT BLANK.

TABLE OF CONTENTS

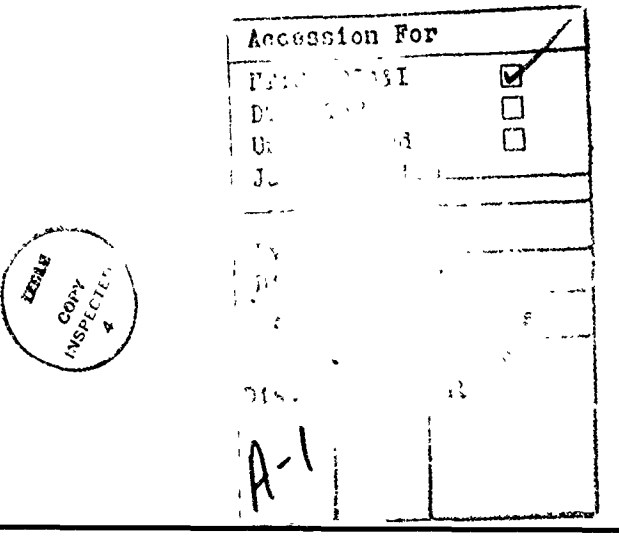

INTENTIONALLY LEFT BLANK.

LIST OF FIGURES

INTENTIONALLY LEFT BLANK.

Acknowledgment

We thank Mr. John Carnahan, Mr. Donald McClellan, Mr. Brendan Patton, and Mr. Andrew McLaughlin for their efforts in setting up the experiment and obtaining the data. We would also like to thank Mr. Douglas Savick, Mr. James Bradley, and Dr. Edward Schmidt for their helpful comments.

INTENTIONALLY LEFT BLANK.

1. INTRODUCTION

1.1 Background. Residents from surrounding communities have complained about gun impulse noise emanating from Army proving grounds. The noise could be reduced by firing from an enclosure to restrict blast wave propagation. The inside surfaces of the enclosure may be as far away as 100 calibers from the weapon muzzle. Designing an enclosure requires an estimate of the forces and impulses on its inside surfaces. By generalizing and extending Smith's work (Smith 1974), BRL developed prediction methods for bare-muzzle guns based on data collected in the range of 10-50 calibers from the gun muzzle (Fansler and Schmidt 1983; Fansler 1985; Heaps et al. 1985). In this approach, the field distance from the muzzle divided by a scaling length is used as the universal independent variable to plot the peak overpressure, etc. This scaling length depends on such parameters as the exit muzzle pressure, exit temperature of the propellant, and the field angular position from the gun bore axis. The resultant predicted free-field muzzle blast can be applied to incident surfaces to obtain the reflected pressures. However, because data were collected for smaller distances, the muzzle blast prediction scheme may not approximate well for the longer distances encountered for the enclosures.

Some investigators have obtained data at greater distances from the muzzle than for the BRL study. Soo Hoo and Moore (1972) primarily studied various naval guns with data taken between 20 and 110 calibers. They obtained pressure contours scaled in terms of calibers applicable to naval guns from 40 mm to 8 inch (203 mm) in bore size. They also obtained data for U. S. Army 20mm M3 and M197 cannon. Naval guns of different bore diameters but having the same barrel length in calibers scaled well over a large range of distances. Scaling for the naval guns was achieved even though the distance in calibers from the ground plane to the muzzle was not constant. However, the different location of the ground-reflecting plane might have significantly reduced correlation for the 20mm cannon data.

Pater (1981) obtained additional data in the far field, and using Soo Hoo and Moore's data, investigated the changing relative angular distribution of the gun blast's shock wave strength with distance. The peak sound pressure level (PSPL) was approximately 23 dB greater at the front than at the rear for the pressure wave front located 20 calibers from the muzzle of a 5 inch/54 naval gun, while in the far field the PSPL difference dropped to 14.3 dB. Schomer et al. (1979) obtained PSPL differences ranging from 14 to 18 dB in the far field. Thus, the muzzle blast decays more rapidly to the front than to the rear.

1.2 Objectives. To assist in the design of blast enclosures, the present study obtains detailed overpressure data over a large range of distances for a tank cannon, firing saboted

projectiles at high velocities and high exit pressures. The data can be coupled with data from small arms to improve the predictive method developed at the BRL (Fansler and Schmidt 1983; Fansler 1985). Also investigated is the development of the propellant gas plume which is correlated with pressure irregularities of the blast wave. A high framing rate camera together with the overpressure data were used to investigate visible features of the muzzle blast.

2. EXPERIMENTAL SET-UP

The experiment was conducted at the BRL Transonic Range with a 105mm M68 tank cannon. The axis of the cannon was nominally horizontal. Firing was done with M735 rounds. The muzzle velocity was approximately 1500 m/s and the muzzle pressure was calculated to be approximately 705 atmospheres.

Nineteen pressure gages were located as shown in Figure 1 at distances from the muzzle ranging from 15 to 400 calibers. Here distance in calibers is simply r divided by the diameter of the cannon bore, D. The gages along the 90° ray were placed at closer intervals to more closely follow the evolution of the blast wave. Seventeen of the gages, obtained from a company called PCB, were mounted in flat disks whose upper surfaces were in the plane that included the direction of the flow from the direct wave toward the gage. Installing the gages in a flat disk with this orientation allowed measuring the static pressure of the direct wave. The resonant frequency of these gages was 250 kHz and the signal rise-time was 2 μs. The diaphragm diameter was 5.5 mm. Two Endevco model 8550M1 microphones were borrowed from Dr. L. Pater, U. S. Army Construction Engineering Research Laboratory (CERL). These microphones, which had a resonant frequency of 60 kHz, are more sensitive than the PCB gages and were placed 150° and 180° from the direction of the fire and 400 calibers from the muzzle. The height of the muzzle was approximately 2 metres above the ground while the gages greater than 50 calibers from the muzzle were approximately 1.2 metres above the ground. The pressure traces were recorded on a Honeywell tape recorder with a frequency response of 80 kHz. Five shots were fired and the signals were later digitized with a Nicolet scope using a sample rate of 5 μs. The time for sampling was 80 ms, which gave sufficient time to observe the complete passage of the wave.

3. RESULTS

For this investigation, three quantities that partially characterize the blast wave were obtained. These quantities are illustrated in Figure 2. The peak overpressure is needed to establish maximum forces and pressures on personnel and equipment. The positive phase duration is needed together with the peak overpressure to calculate the impulse given to structures. The time of arrival is needed to establish the shape of the blast wave and from this the incidence angle of a wave upon a reflecting surface.

3.1 Peak Overpressure. The ground plane produces a reflected wave that interferes with the direct wave, which is of primary interest. Where there was not complete certainty that the direct wave value had been obtained, that value was categorized as of questionable validity. The data for the direct waves that have merged with the reflected waves were discarded.

3.1.1 Basic Data Presentation. Figure 3 shows the overpressure-time curve along the 90° ray at a distance from the muzzle of $r/D = 15$. The main wave has superimposed upon it small-amplitude high-frequency randomized oscillations that decrease in amplitude with time. This noise is thought to be caused by turbulent processes in the blast wave and during blow-down of the gun tube. The reflected wave occurs late enough that the direct wave's development in the positive phase of the overpressure is not obscured by reflections.

Figure 4 portrays the overpressure-time curve along the 90° ray 400 calibers from the muzzle. The noise superimposed upon the wave is greatly reduced at these longer distances and arises from the higher attenuation of high-frequency signals travelling through the air. The ground reflection is observed to immediately follow the primary blast. The peak overpressure and time-of-arrival data are not degraded by the reflected wave but the positive-phase-duration data must be thrown away.

Examples of overpressure wave data obtained at the front and the back of the cannon are given in Figure 5 and Figure 6. The wave obtained at the front of the gun has a secondary peak superimposed on its underpressure phase. The front of the reflected wave follows closely behind the direct wave's shock wave in both figures but it is thought that the reflected wave has not increased the peak value of the direct wave. Figure 7 shows an example of a merged wave that must be excluded from the good data. Most of the peak overpressure and time-of-arrival data were usable for building an improved muzzle blast prediction method.

The peak overpressure data for 30, 100, and 400 calibers are plotted in Figure 8 as a

function of polar angle from the bore-line. For comparison the predicted values are shown also. The prediction for 30 calibers shows good agreement although the predicted values are all less than the observed values. The predicted values at the other distances decrease too rapidly with increasing angle, reflecting that the measured front-to-back ratios of blast wave strength decreases with distance, as other experimenters have observed (Pater 1981; Soo Hoo and Moore 1972). Figure 9 shows peak overpressure versus distance in calibers. To the front, the peak overpressures decline faster than predicted. To the rear, the peak overpressures decline slower than predicted. The rate of peak overpressure decline with distance is in qualitative agreement with blast wave calculations and data obtained for spherical blast waves.

3.1.2 Scaled Data Presentation. The distance from the muzzle can be nondimensionalized by the scaling length referred to earlier (Heaps et al. 1985), and the resulting data plotted. Figure 10 shows the peak overpressure versus the scaled distance and the predicted curve. The data is separated into categories of good and questionable. The questionable data corresponds to primary blast waves that are obscured greatly by ground reflections. The nondimensionalized distances span a large range.

3.1.3 Comparison with Other Data and Prediction. Some of the data used in developing the prediction method were used to compare with the present data and the prediction. The combined data are shown as a function of scaled distance in Figure 11. Comparisons between the old and new data show agreement. The new data show noticeably worse agreement at two locations.

3.2 Time of Arrival. The time of arrival is plotted versus the distance for different values of the polar angle, θ, in Figure 12. The data are presented without utilizing the scaling length since a correction term that accounts for the blast apparently coming from a center forward of the muzzle destroys the strict scaling (Fansler and Schmidt 1983). Further scaling analysis of the time-of-arrival data will be done when more blast data are collected.

3.3 Positive Phase Duration. Because of interference by the reflected wave, the positive-phase-duration data for this experiment are restricted to the positions close to the muzzle. Figure 13 shows the positive phase duration as a function of the distance in calibers, with the polar angle as the parameter. Because of wave reflection from the ground, little valid data were obtained. Nevertheless, the data were obtained close to the muzzle of a gun

with high-velocity high-muzzle-pressure conditions. No other data will be obtained for these ballistic conditions.

3.4 Wave Anomalies. For some probe positions, the blast wave signatures included a precursor portion. Examples of precursor waves can be seen in Figure 6 and Figure 7. These precursor waves were analyzed and possible hypotheses were developed, such as the possibility that the precursor generated by the projectile in-bore would not be overtaken by the main blast wave. The predictive model was used to obtain time of arrival for both the precursor blast and the main blast. The predictive model showed that the main blast wave overtakes the precursor wave for the locations of interest. We also investigated whether there might be crosstalk between signal lines. Crosstalk was ruled out but we can find no other plausible explanation for the precursor signals.

Figure 14 shows time of arrival versus polar angle at 100 calibers for both the main blast and the precursor wave. The precursor arrival times do not always diminish with smaller values of the polar angle as occurs for main blast arrival times. Figure 15 shows the time-of-arrival data at 400 calibers. For larger angles, the precursor seems to be travelling slower than the front of the main blast wave. Since the amplitude of the precursor wave is smaller, the precursor should be travelling with less velocity than the main blast wave, if the two waves are independent. However, no such clear trend is seen for the smaller angles.

Figure 16 shows all the precursor data as a function of r/D, where the time of arrival is nondimensionalized by the ambient speed of sound divided by the bore diameter, D. The data show the precursor wave travelling at approximately the speed of sound, which is expected for these small-amplitude waves.

The blast wave signatures all have high-frequency waves – that for the most part appear random – superimposed upon the basic shape. However, almost all have a distinct positive-going pulse appearing sometime after the front of the wave passes. Figures 4 and 5 both clearly show these positive-going pulses. Figure 17 shows a comparison between the time of arrival for the main blast and the positive-pressure pulses. The times of arrival are again multiplied by the ambient speed of sound divided by D to obtain nondimensionalized quantities. The time-of-arrival differences increase to the front with distance but decrease to the rear. The main wave travel speed could account for this difference to the front. If the origin of the pressure pulse is in front of the origin of the main blast, the time-of-arrival differences could decrease to the sides. However, there is no clear explanation for the difference decrease at 180°.

It was originally thought that the pulse might be caused by secondary flash. Accordingly,

the high-framing-rate camera data were used to outline the boundaries of the propellant gas and incandescence. Photographs of the firings show that the propellant gas exiting the tube is incandescent. The propellant gas expands forward for several metres, still in an incandescent condition. Finally, the propellant gas burns with diminishing intensity starting from the rear and with the incandescent boundary moving forward. Where burning has ceased in the propellant gas, smoke remains in the same volume. Figure 18 shows the top and bottom boundaries of propellant gas and incandescence. The bottom boundary is limited in its movement by the ground. The velocity of the top boundary decreases until around 7 *ms* where it abruptly increases but then declines monotonically. This velocity increase may be caused by the reflection of pressure waves from the ground plane. Figure 19 shows the front and rear boundaries of the incandescent material. Again the boundary appears to speed up at around 7 *ms*. This velocity increase could send out a pressure pulse superimposed upon the wave. Thus this velocity increase does not appear to be connected with secondary flash as originally thought but rather with the partial confinement of the propellant exhaust plume by the ground plane. The time for the pulse to be sent out is generally consistent with the data obtained in Figure 17.

4. SUMMARY AND CONCLUSIONS

Blast wave data were obtained around a tank gun weapon at a large range of distances and angles to add to a muzzle blast database. The completed database will be used to improve the present prediction method. With a reduced-scale tank cannon, the ground plane could have been located far enough away to reduce the influence of the reflected wave. Since the cost would have been prohibitive to build a reduced-scale model, a 105 mm cannon was used to fire M735 projectiles.

Five firing records were obtained from 19 pressure gages. The peak overpressure, time-of-arrival, and positive-phase-duration data were obtained and presented. The front-to-back peak overpressure dB differences decreased with distance, as other investigators have noted. The amount of usable positive-phase-duration data were limited by interfering waves reflecting from the ground plane. The data for the various quantities were used to compare with the predicted values.

Some wave anomalies were investigated. The precursor signals were travelling at a lower velocity than the main blast wave front for the larger polar angles. Lower velocities were expected - the precursor shock wave front has a smaller shock strength than the main wave blast front - since waves with lower shock strength travel slower. However, this trend was not observed for the smaller polar angles and the existence of these precursor shock waves cannot

be plausibly explained. The positive pulse occurring during the wave's underpressure phase is thought to be caused by the confinement of the exhaust plume by the ground. The next planned series of tests are designed to minimize blast wave interaction with the ground plane. To see if the precursor and positive-pressure waves are cause by ground-plane interactions, we will search for their existence in the next test series.

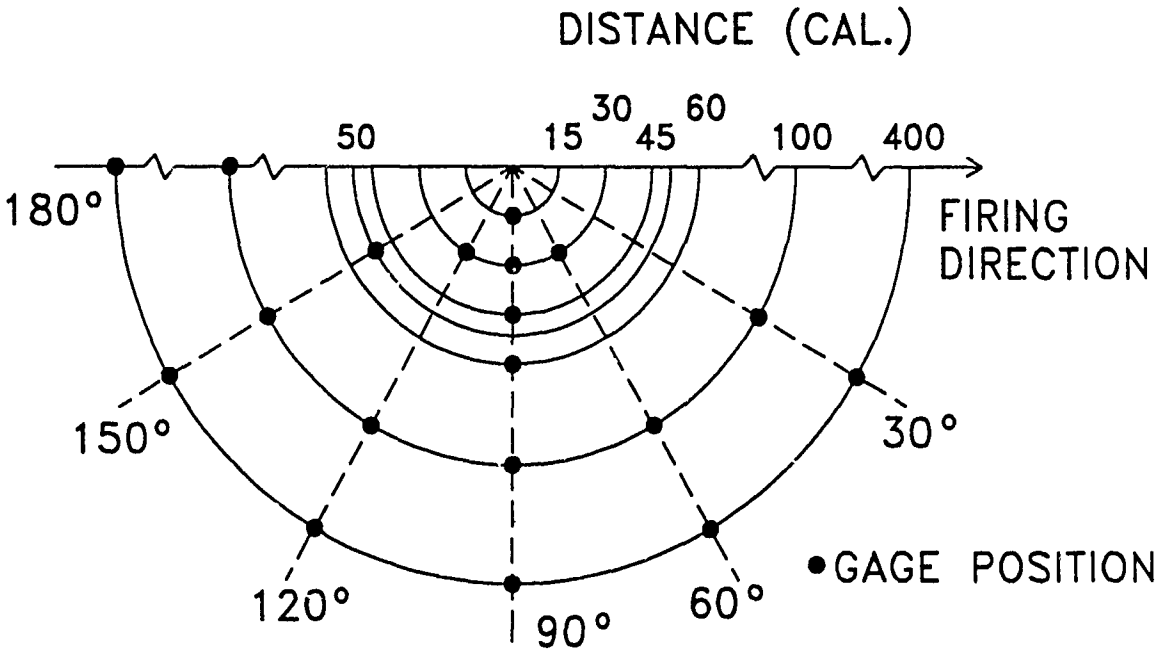

Figure 1. Schematic of Test Set-Up.

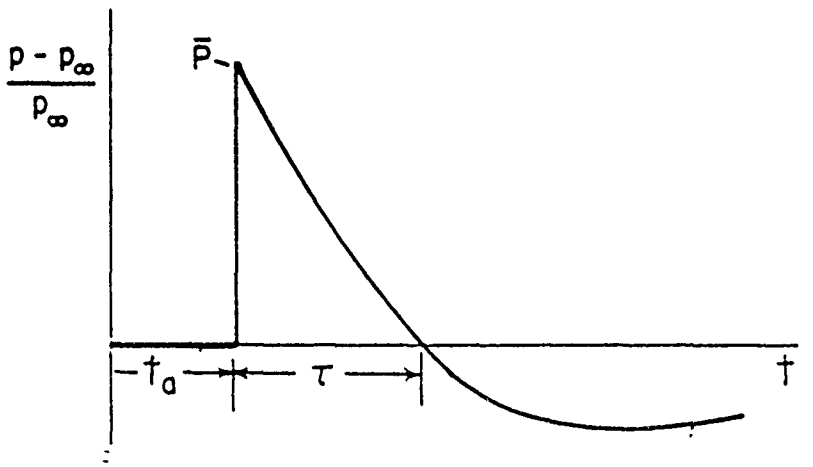

- PEAK OVERPRESSURE, $\overline{P}$
- TIME OF ARRIVAL, t_a
- POSITIVE PHASE DURATION, τ

Figure 2. Illustration of Blast Wave Quantities; Peak Overpressure, Time of Arrival, and Positive Phase Duration.

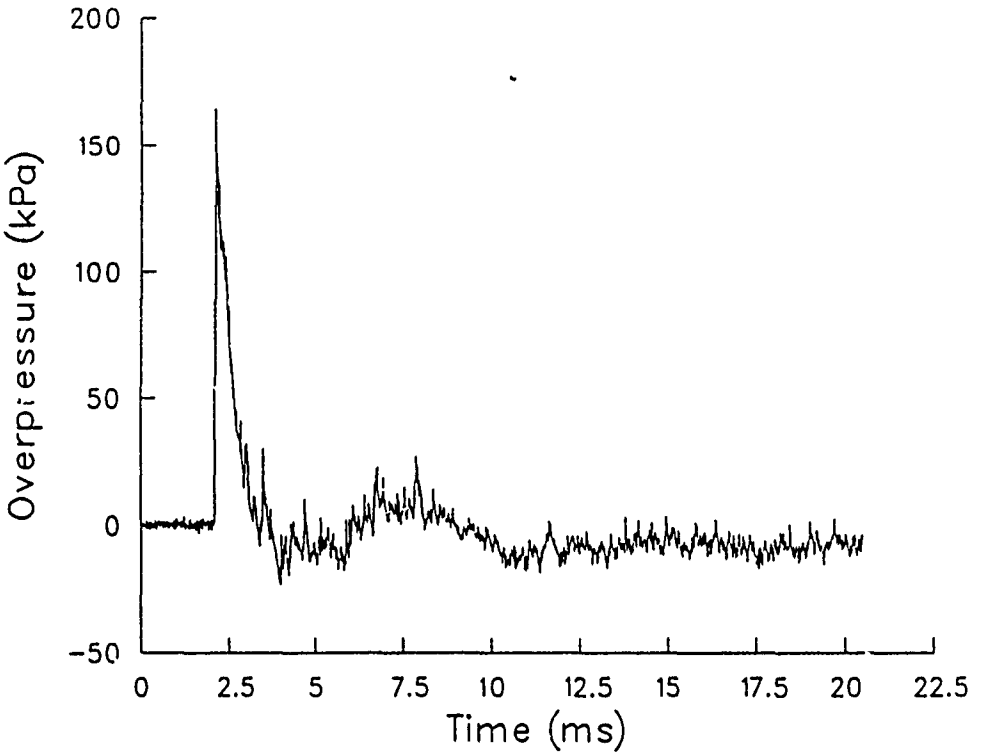

Figure 3. Overpressure vs. Time, $\theta = 90°, r/D = 15$.

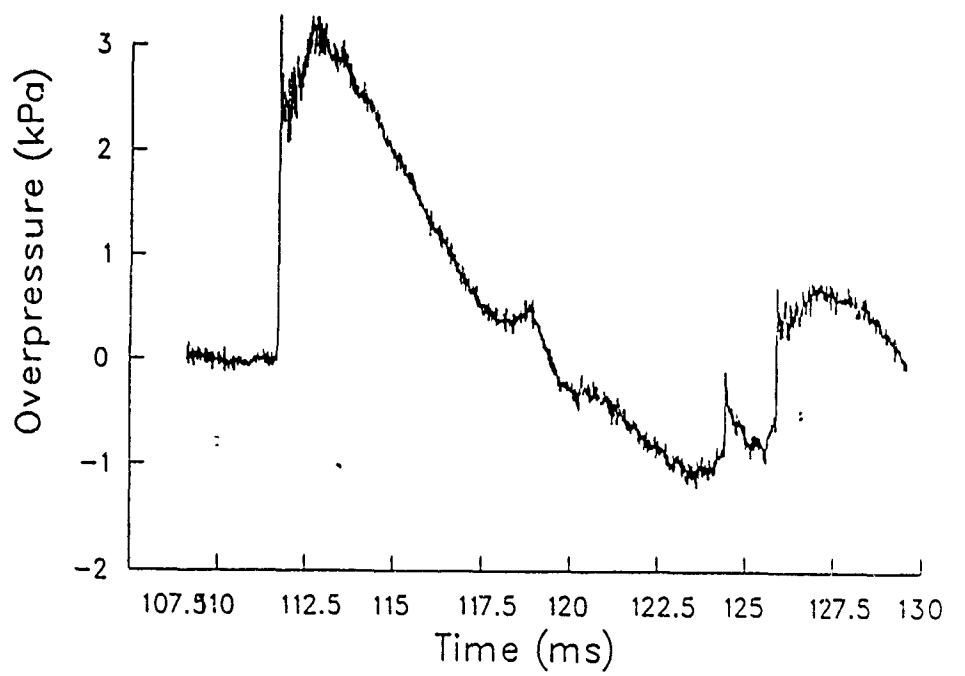

Figure 4. Overpressure vs. Time, $\theta = 90°, r/D = 400$.

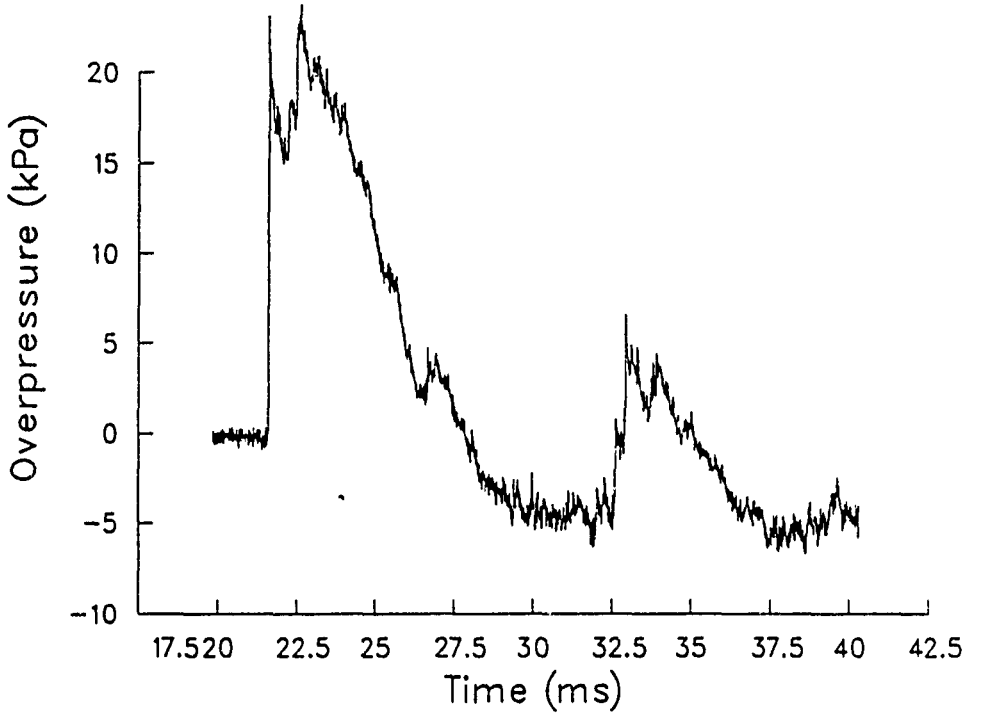

Figure 5. Overpressure vs. Time, $\theta = 60°, r/D = 100$.

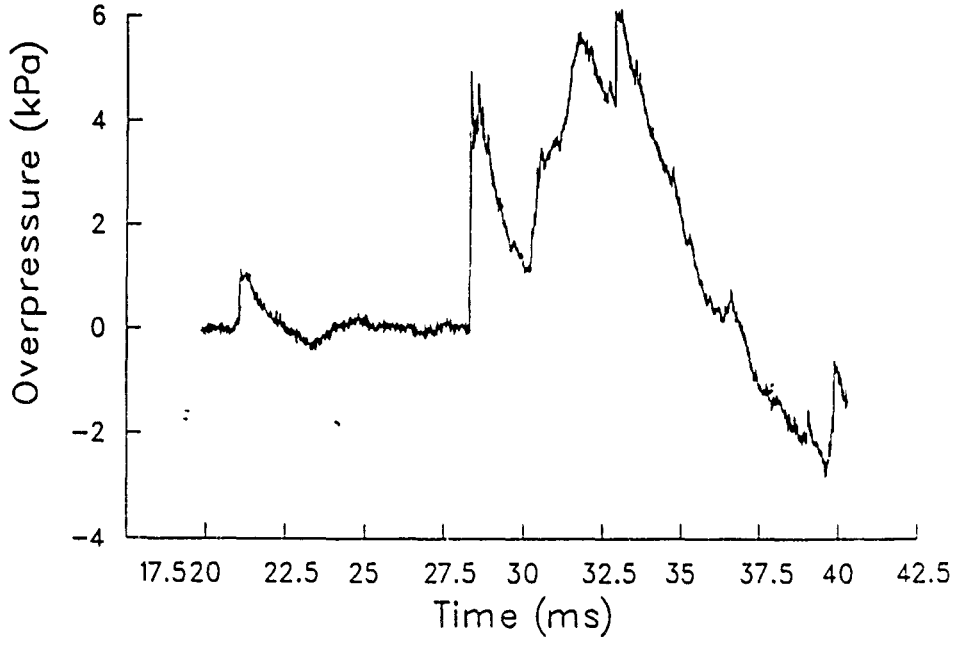

Figure 6. Overpressure vs. Time, $\theta = 180°, r/D = 100$.

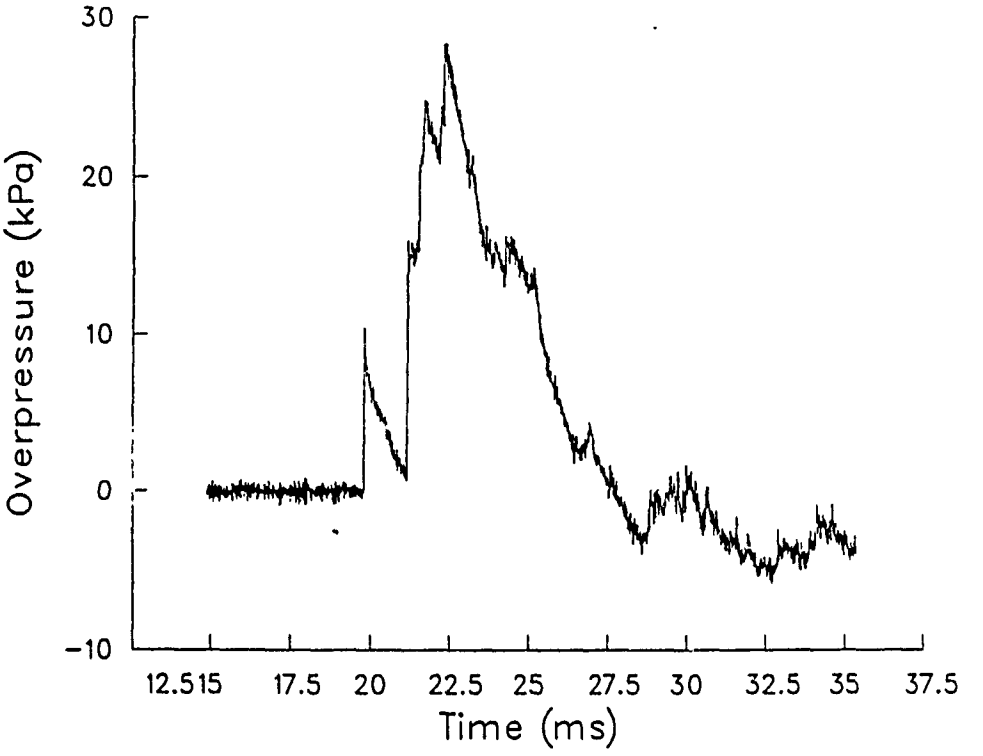

Figure 7. Direct Wave Merged with Reflected Wave, $\theta = 30°, r/D = 100$.

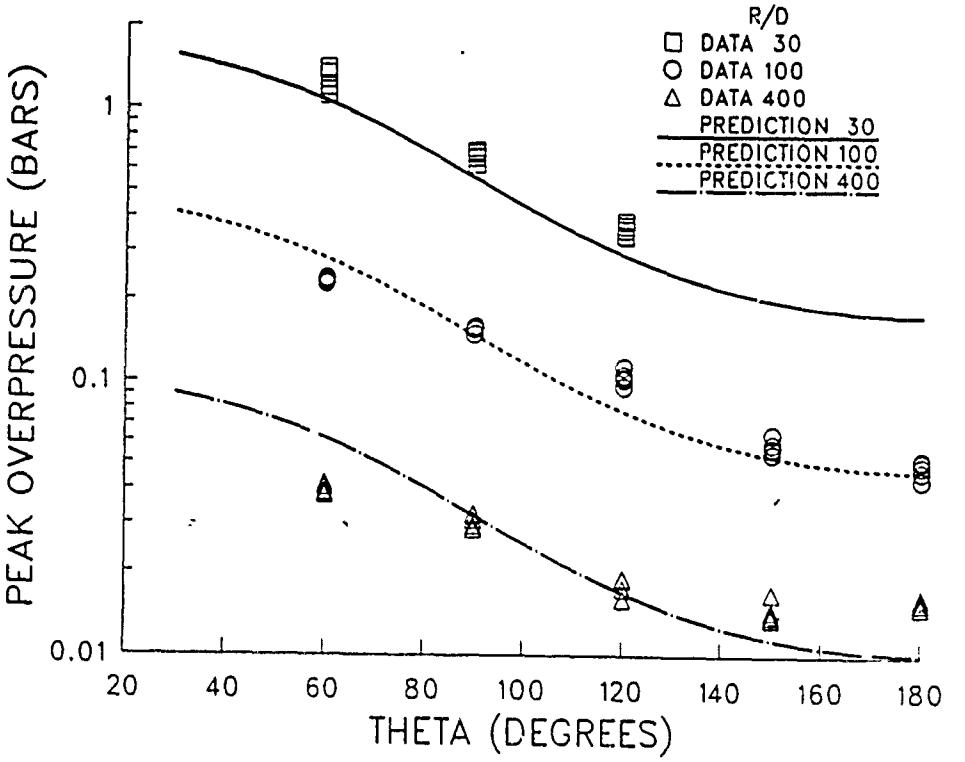

Figure 8. Peak Overpressure vs. Polar Angle.

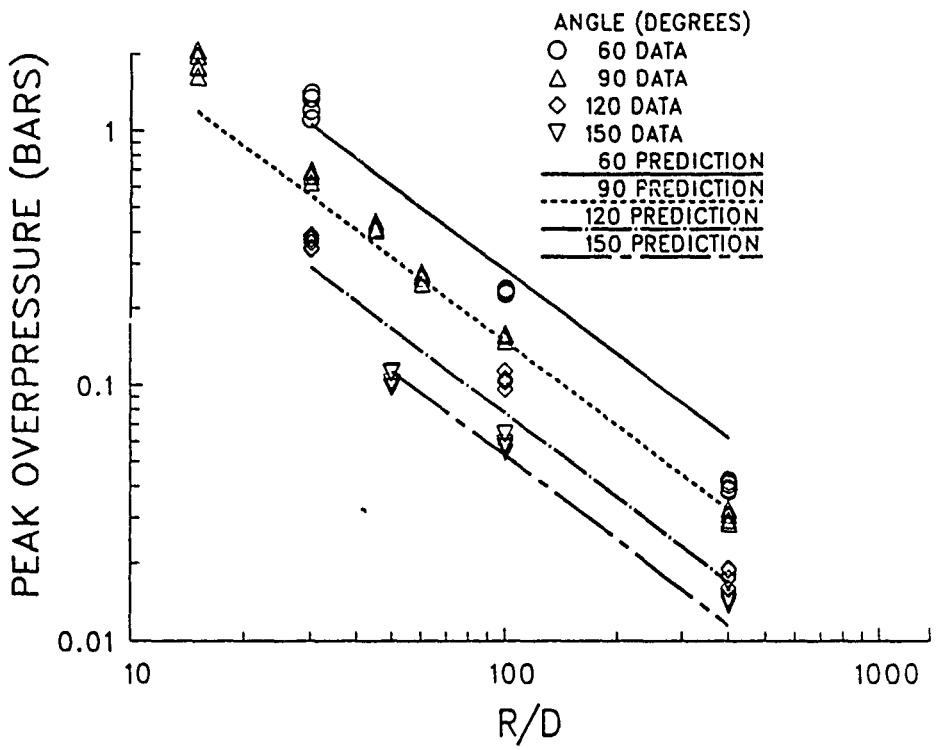

Figure 9. Peak Overpressure vs. r/D.

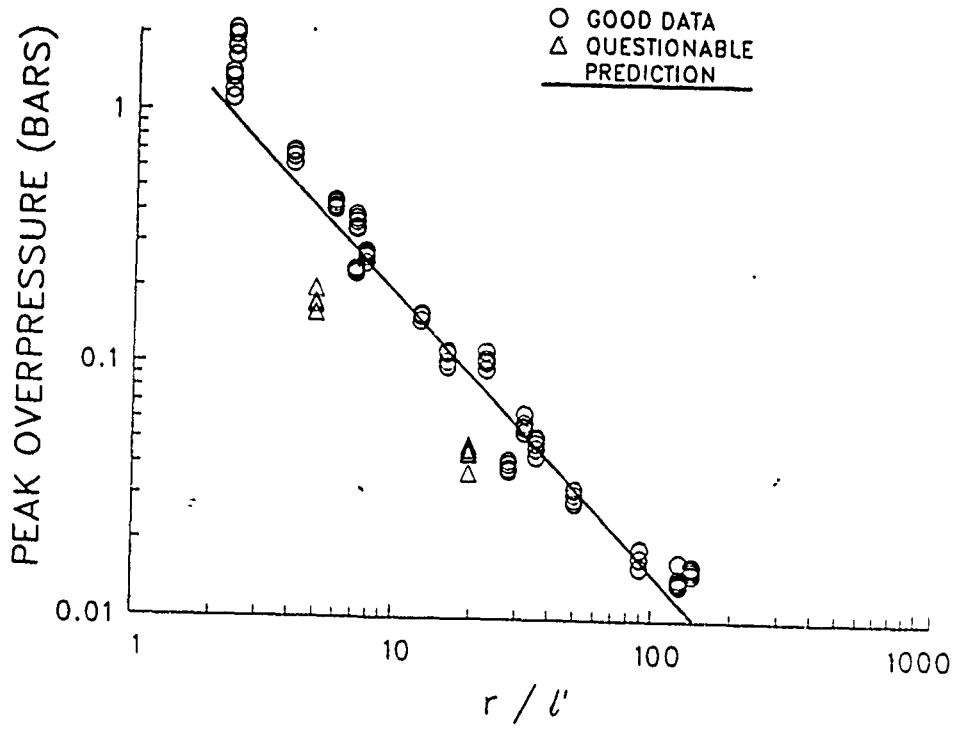

Figure 10. Comparison of Peak Overpressure Data with Prediction.

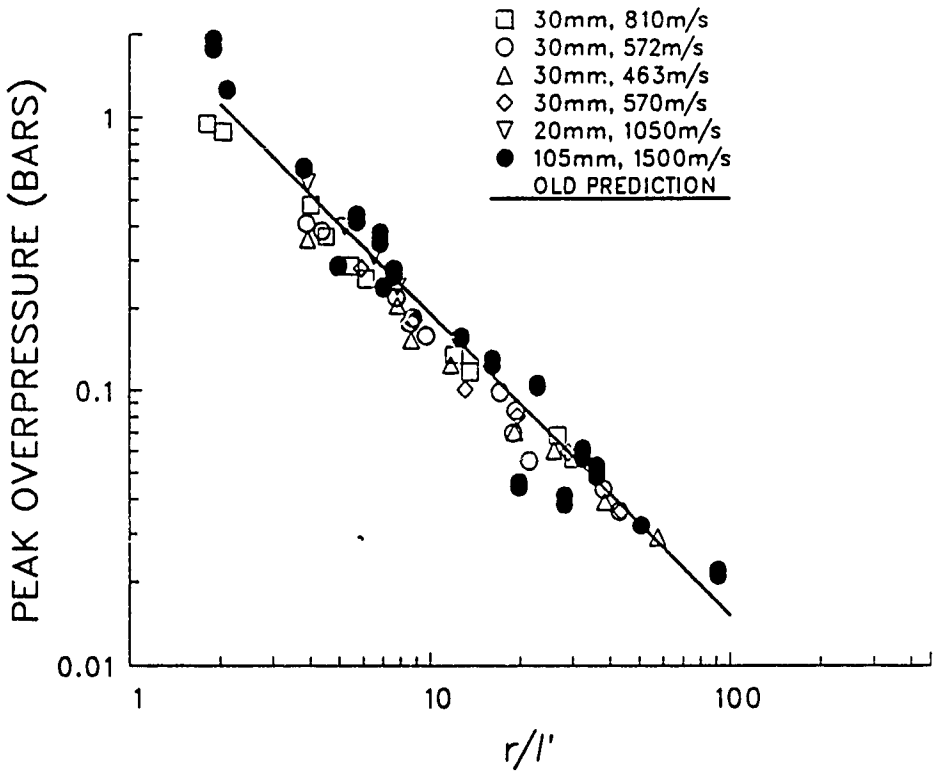

Figure 11. Combined Old and New Data Compared with Prediction.

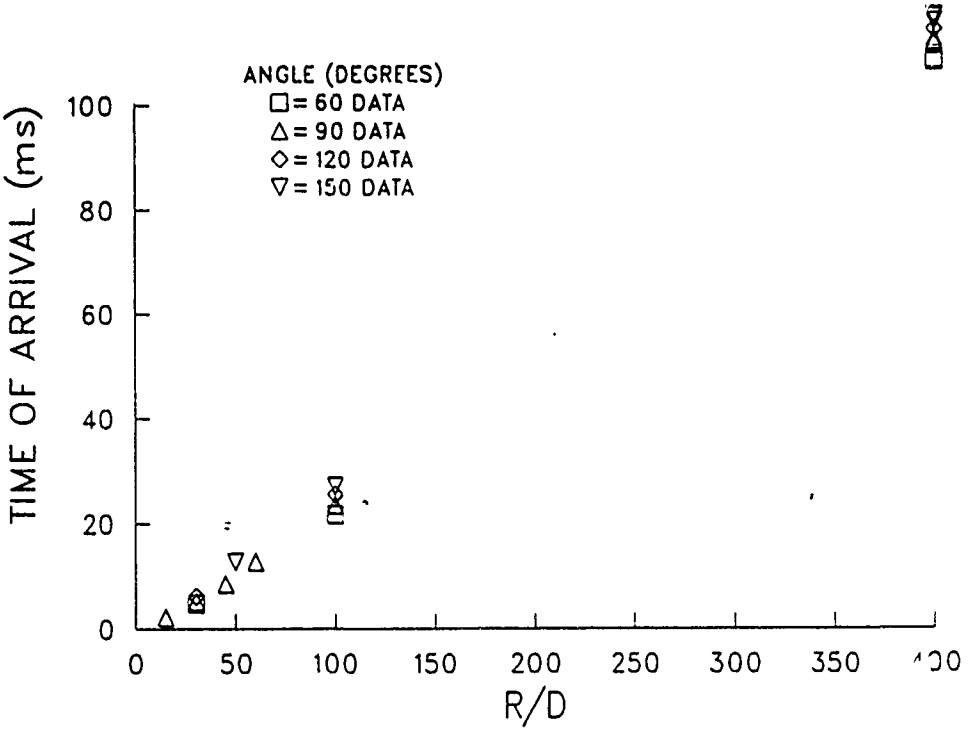

Figure 12. Time of Arrival vs. r/D for Main Blast Wave.

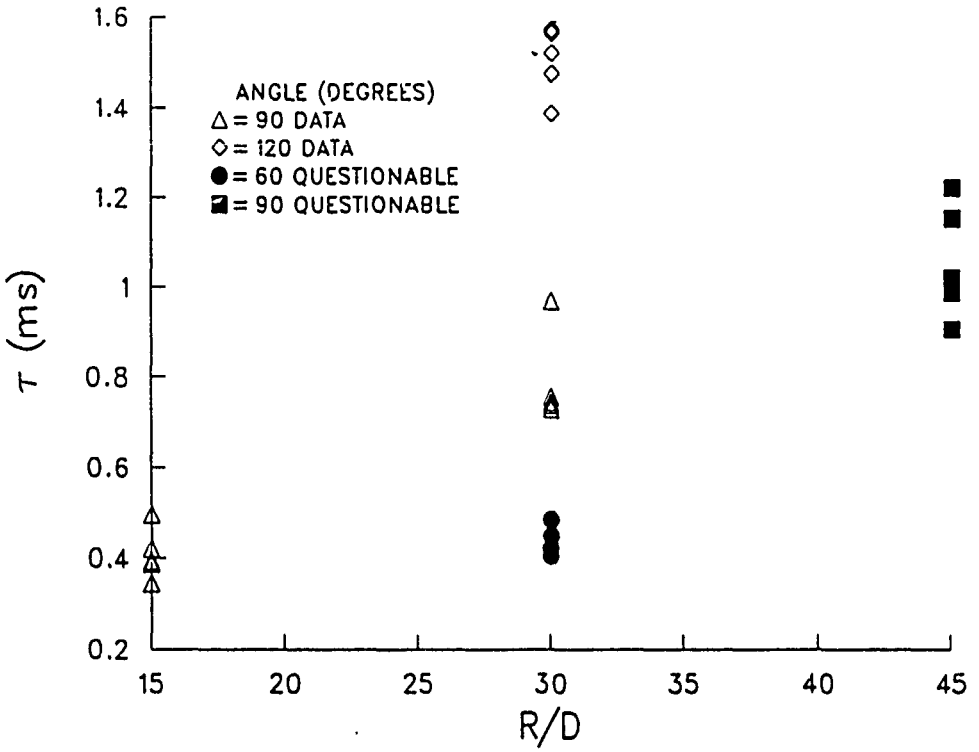

Figure 13. Positive Phase Duration vs. Distance.

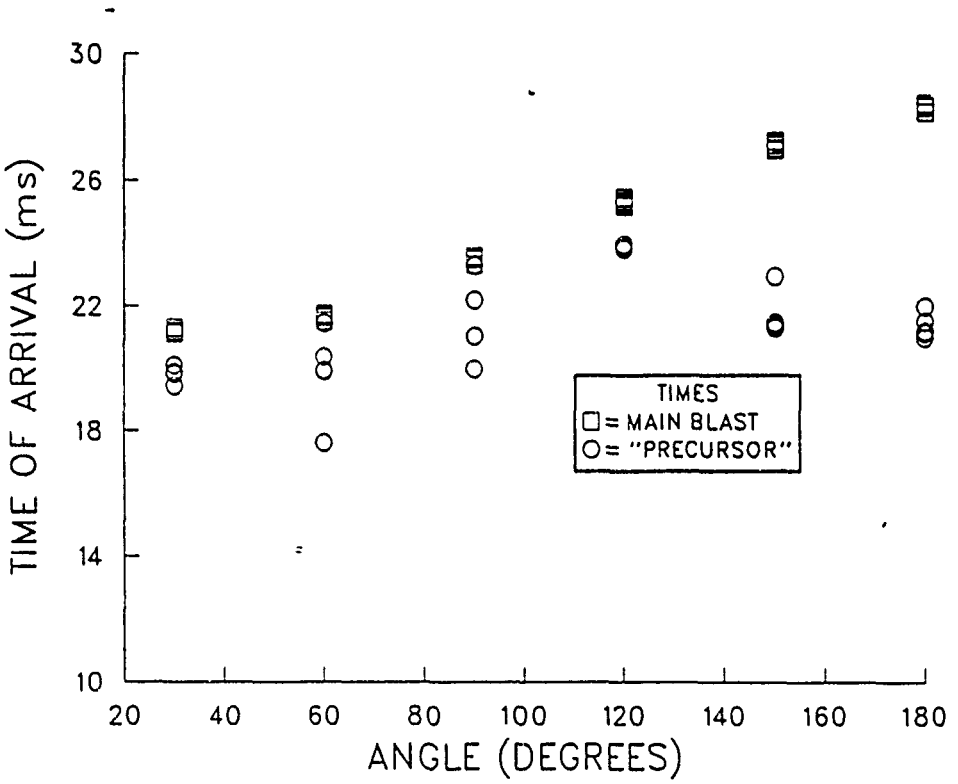

Figure 14. Precursor and Main-Blast Times of Arrival vs. Polar Angle, $r/D = 100$.

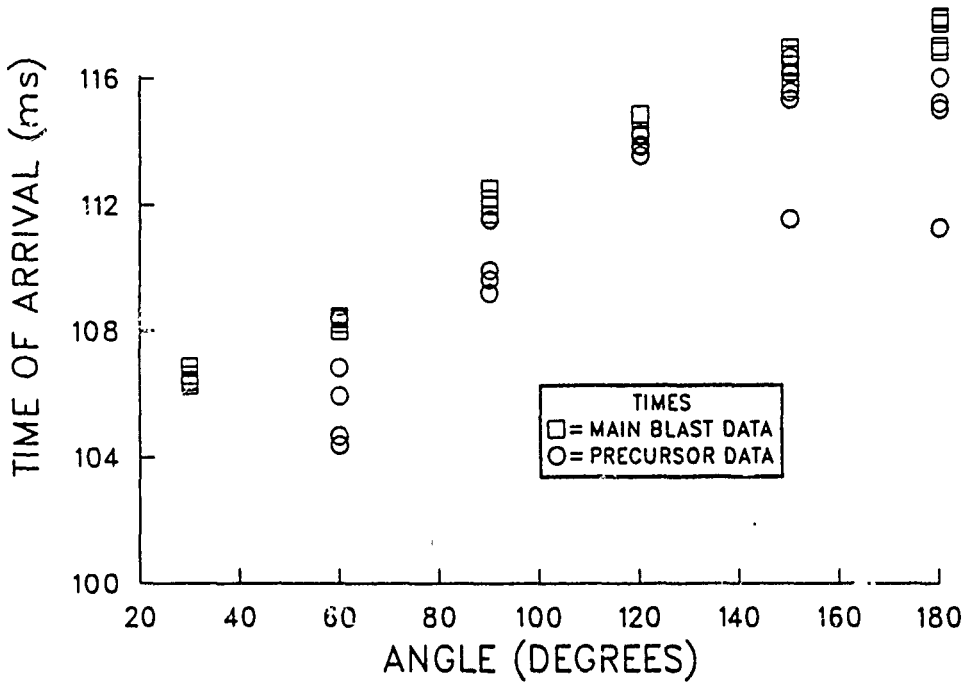

Figure 15. Precursor and Main-Blast Times of Arrival vs. Polar Angle $r/D = 400$.

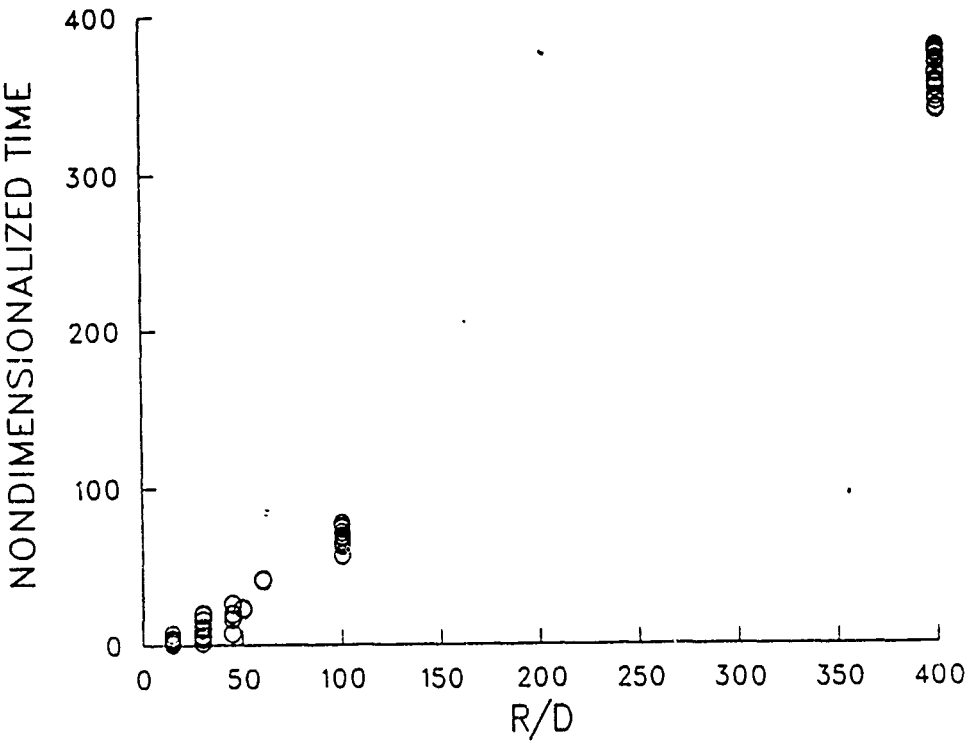

Figure 16. Precursor Time of Arrival vs. r/D, Time Nondimensionalized by Multiplying by a_∞/D.

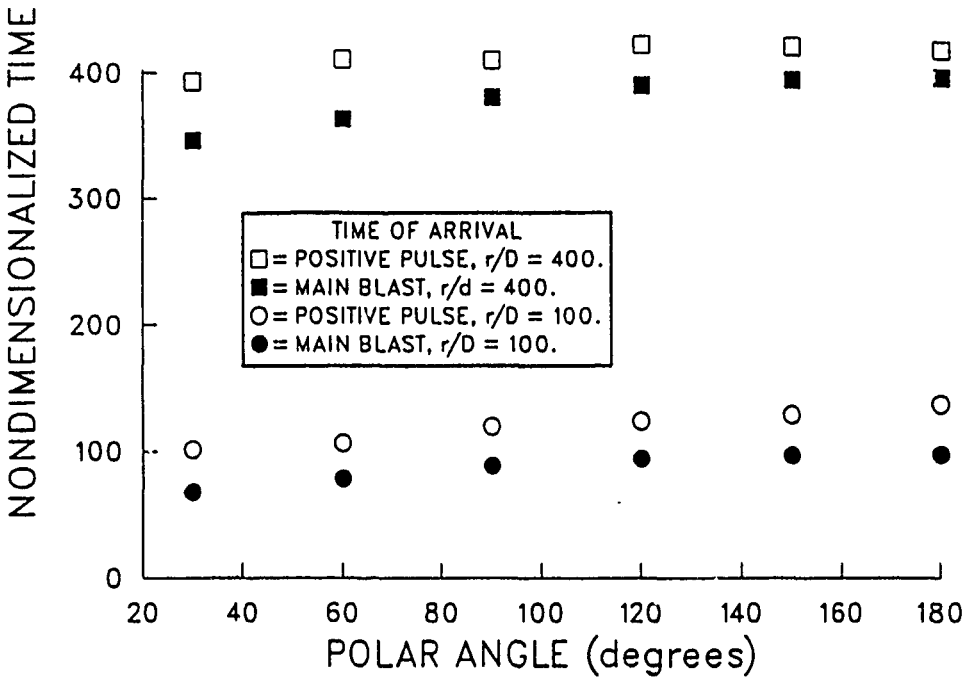

Figure 17. Comparisons between the Main Blast and the Pressure Pulse, Nondimensionalized Arrival Time vs. Polar Angle.

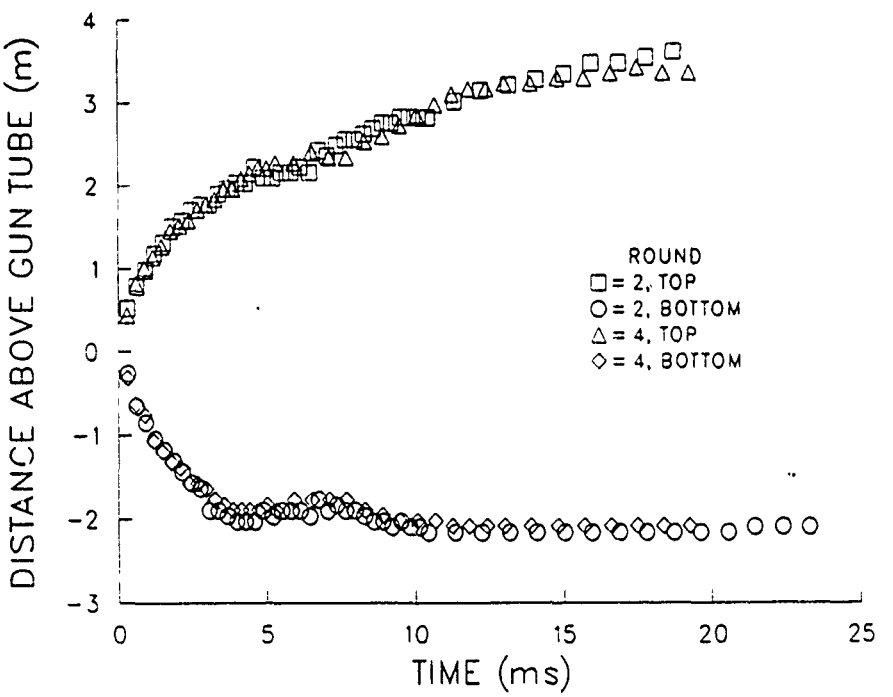

Figure 18. Top and Bottom Boundaries of Propellant Gas.

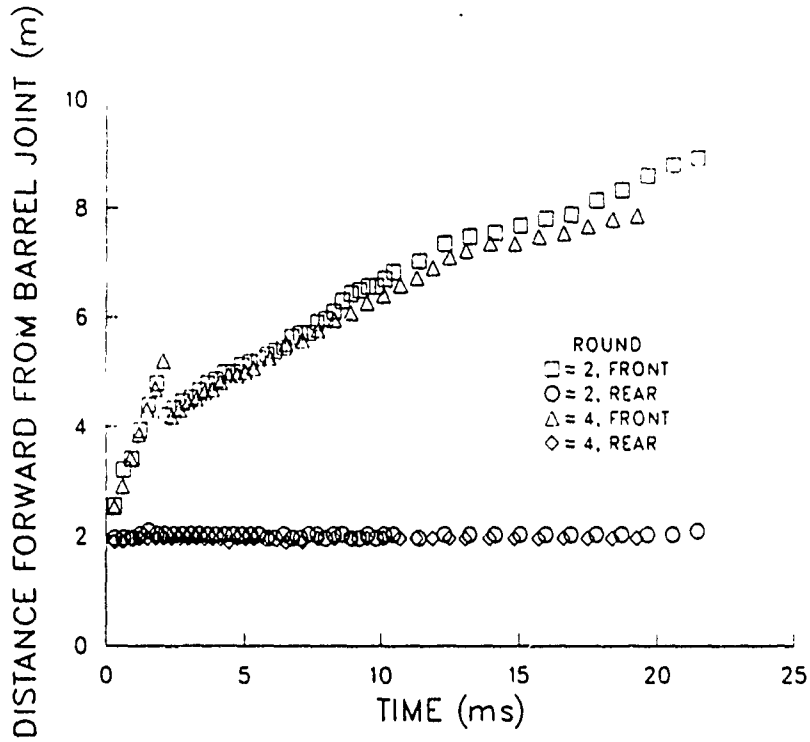

Figure 19. Front and Rear Boundaries of Propellant Gas.

INTENTIONALLY LEFT BLANK.

5. REFERENCES

AMCP 706-181. See also "Department of Defense."

Department of Defense. "*Engineering Design Handbook, Explosions in Air, Part I.*" U.S. Army Materiel Command, AMCP 706-181, Washington, D.C. (Write: NTIS, Department of Commerce, Springfield, VA 22151), 1974.

Fansler, K. S. and E. M. Schmidt. "The Prediction of Gun Muzzle Blast Properties Utilizing Scaling." ARBRL-TR-02504, U.S. Army Ballistic Research Laboratory, Aberdeen Proving Ground, Maryland, July 1983. (AD B07859)

Fansler, K. S. "Dependence of Free Field Impulse on the Decay Time of Energy Efflux for a Jet Flow." *The Shock and Vibration Bulletin*, Part 1, published by The Shock and Vibration Center, Naval Research Laboratory, 22-24 October, 1985, pp. 203-212.

Heaps, C. W., K. S. Fansler, and E. M. Schmidt. "Computer Implementation of a Muzzle Blast Prediction Technique." ARBRL-MR-3443, U.S. Army Ballistic Research Laboratory, Aberdeen Proving Ground, Maryland, May 1985. (AD A158344)

Pater, L. L. "Gun Blast Far Field Peak Overpressure Contours." Naval Surface Weapons Center, Dahlgren, VA, TR 79-442, March 1981.

Schomer, P. D., L. M. Little, and A. D. Hunt. "Acoustic Directivity Patterns for Army Weapons." Interim Report N-60, U. S. Army Construction Engineering Research Laboratory, Champaign, IL, January 1979.

Smith, F. "A Theoretical Model of the Blast from Stationary and Moving Guns." *First International Symposium on Ballistics*, Orlando, Florida, 13-15 November 1974.

Soo Hoo, G. and G. R. Moore. "Scaling of Naval Gun Blast Peak Overpressures." Naval Surface Weapons Center, Dahlgren, VA, TN-T7-72, August 1972.

INTENTIONALLY LEFT BLANK.

No. of Copies	Organization
2	Administrator Defense Technical Info Center ATTN: DTIC-DDA Cameron Station Alexandria, VA 22304-6145
1	Commander U.S. Army Materiel Command ATTN: AMCAM 5001 Eisenhower Avenue Alexandria, VA 22333-0001
1	Commander U.S. Army Laboratory Command ATTN: AMSLC-DL 2800 Powder Mill Road Adelphi, MD 20783-1145
2	Commander U.S. Army Armament Research, Development, and Engineering Center ATTN: SMCAR-IMI-I Picatinny Arsenal, NJ 07806-5000
2	Commander U.S. Army Armament Research, Development, and Engineering Center ATTN: SMCAR-TDC Picatinny Arsenal, NJ 07806-5000
1	Director Benet Weapons Laboratory U.S. Army Armament Research, Development, and Engineering Center ATTN: SMCAR-CCB-TL Watervliet, NY 12189-4050
(Unclass. only) 1	Commander U.S. Army Armament, Munitions and Chemical Command ATTN: AMSMC-IMF-L Rock Island, IL 61299-5000
1	Director U.S. Army Aviation Research and Technology Activity ATTN: SAVRT-R (Library) M/S 219-3 Ames Research Center Moffett Field, CA 94035-1000

No. of Copies	Organization
1	Commander U.S. Army Missile Command ATTN: AMSMI-RD-CS-R (DOC) Redstone Arsenal, AL 35898-5010
1	Commander U.S. Army Tank-Automotive Command ATTN: ASQNC-TAC-DIT (Technical Information Center) Warren, MI 48397-5000
1	Director U.S. Army TRADOC Analysis Command ATTN: ATRC-WSR White Sands Missile Range, NM 88002-5502
1	Commandant U.S. Army Field Artillery School ATTN: ATSF-CSI Ft. Sill, OK 73503-5000
(Class. only) 1	Commandant U.S. Army Infantry School ATTN: ATSH-CD (Security Mgr.) Fort Benning, GA 31905-5660
(Unclass. only) 1	Commandant U.S. Army Infantry School ATTN: ATSH-CD-CSO-OR Fort Benning, GA 31905-5660
1	Air Force Armament Laboratory ATTN: WL/MNOI Eglin AFB, FL 32542-5000
	Aberdeen Proving Ground
2	Dir, USAMSAA ATTN: AMXSY-D AMXSY-MP, H. Cohen
1	Cdr, USATECOM ATTN: AMSTE-TC
3	Cdr, CRDEC, AMCCOM ATTN: SMCCR-RSP-A SMCCR-MU SMCCR-MSI
1	Dir, VLAMO ATTN: AMSLC-VL-D
10	Dir, BRL ATTN: SLCBR-DD-T

No. of Copies	Organization
1	Commander United States Army, Europe ATTN: AEAGC-TD-TM, SFC C. Hutchinson APO NY 09114-5413
1	Commander HQ AMC, Europe ATTN: AMXEU-SA, R. Gilbert APO New York 09333-4747
1	Commander HQ United States Army, Europe ATTN: AEAGX-CS, A. Christensen Heidelberg APO NY 09403
1	Commander HQ AMC, Europe ATTN: AMXEU-SA, T. Stevenson APO New York 09333-4747
1	Commander US Army Armament, Munitions and Chemical Command ATTN: AMSMC-LEP-L Rock Island, IL 61299-5000
1	Commander US Army Missile Command ATTN: AMSMI-RD, Dr. W. Walker Redstone Arsenal, AL 35898-5000
1	Director US Army Missile & Space Intelligence Center ATTN: AIAMS-YDL Redstone Arsenal, AL 35898-5000
3	Commander US Army Watervliet Arsenal ATTN: SMCWV-QAR, T. McCloskey SMCWV-ODW, T. Fitzpatrick SMCWV-ODP, G. Yarter Watervliet, NY 12189
1	Commander AMC-FAST Office ATTN: AMSLC-SA, R. Franseen Fort Belvoir, VA 22060-5606

No. of Copies	Organization
7	Commander US Army Armament RD&E Center ATTN: SMCAR-FS, Dr. Davidson SMCAR-FSA, Mr. Wrenn SMCAR-CC, Mr. Hirshman SMCAR-CCH, Mr. Moore SMCAR-CCL, Mr. Gehbauer E. Seeling J. Donham Picatinny Arsenal, NJ 07801-5000
2	Commander US Army Tank Automotive Command ATTN: AMCPM-BFVS ATTN: AMCPM-BFVS-SC, K. Pitco Warren, MI 48397-5000
1	Commander US Army Research Office P.O. Box 12211 Research Triangle Park, NC 27709
2	Commandant US Army Infantry School ATTN: ATSH-IV-SD, R. Gorday ATSH-TSM Fort Benning, GA 31905-5660
1	Commander ATTN: AEAGC-ATC-TS, P. Minton USAREUR, Grafenwoehr, FRG APO, NY 09114
6	Director Benet Weapons Laboratory U. S. Armament Research, Development, and Engineering Center ATTN: SMCAR-CCB, J. Bendick T. Simkins SMCAR-CCB-DS, P. Vottis SMCAR-CCB-DS, C. Andrade SMCAR-CCB-RA, G. Carofano SMCAR-CCB-RA Watervliet, NY 12189-4050

No. of Copies	Organization
1	Commander Tank Main Armament Systems ATTN: AMCPM-TMA, R. Billington Picatinny Arsenal, NJ 07806-5000
3	Department of the Army Construction Engineering Research Laboratory ATTN: CERL-SOI, P. Schomer L. Pater J. Wilcoski P. O. Box 4000 Champaign, IL 61820
1	Commander (Code 3433) Naval Warfare Center ATTN: Tech Lib China Lake, CA 93555
1	Commander US Naval Air Systems Command ATTN: AIR-604 Washington, DC 20360
2	Commander Naval Surface Warfare Center ATTN: 6X, J. Yagla G. Moore Dahlgren, VA 22448
1	Commander (Code 3892) Naval Warfare Center ATTN: K. Schadow China Lake, CA 93555
1	Commander (Code 730) Naval Surface Weapons Center Silver Spring, MD 20910
1	Director NASA Scientific & Technical Information Facility ATTN: SAK/DL P. O. Box 8757 Baltimore/Washington International Airport, MD 21240
1	McDonnell Douglas ATTN: Joseph Smuckler 1014 Ferngate Lane Creve Coeur, MO 63141

No. of Copies	Organization
2	Alliant Techsystems Inc. ATTN: MS MN 50-2060, T. Melanger S. Langley 600 Second Street, Northeast Hopkins, MN 55343
1	S & D Dynamics, Inc. ATTN: R. Becker 7208 Montrico Dr Boca Raton, FL 33433-6930
1	AAI Corporation ATTN: T. Stasney J. Hebert P. O. Box 126 Cockeysville, MD 21030
3	Aerojet General Corporation ATTN: W. Wolterman S. Rush A. Flatau P.O. Box 296 Azusa, CA 91702
1	Lockheed Aircraft, Inc. ATTN: J. Brown P. O. Box 33, Dept. 1-330/UPLAND Ontario, CA 91761
2	United Technologies Corporation Chemical Systems Division ATTN: R. MacLaren A. Holzman P. O. Box 49028 San Jose, CA 95150-0015
1	General Electric Armament & Electric Systems ATTN: R. Whyte Lakeside Avenue Burlington, VT 05401
1	Director Sandia National Laboratories ATTN: Aerodynamics Dept, Org 5620, R. Maydew Albuquerque, NM 87115

No. of Copies	Organization
1	Franklin Institute ATTN: Tech Library Race & 20th Streets Philadelphia, PA 19103
1	Director Applied Physics Laboratory The Johns Hopkins University Johns Hopkins Road Laurel, MD 20707
2	Loral Corporation ATTN: S. Schmotolocha B. Axely 300 N. Halstead St. P. O. Box 7101 Pasadena, CA 91109
1	Martin Marietta Aerospace ATTN: A. Culotta P. O. Box 5837 Orlando, FL 32805
2	McDonnell Douglas Helicopter Co. ATTN: D. Van Osteen R. Waterfield Mail Station D216 500 E. McDowell Rd. Mesa, AZ 85205
1	FMC Corporation Advanced Systems Center ATTN: S. Langlie 1300 South Second St. P. O. Box 59043 Minneapolis MN 55459
1	Red Eye Arms, Inc. ATTN: David Byron Gunn Station 507 N. New York Ave. Winter Park, FL 32789
1	FN Manufacturing, Inc. ATTN: George Kontis Post Office Box 24257 Columbia, SC 29224
1	Old Dominion University Mathematics Department ATTN: Dr. Charlie Cooke Norfolk, VA 23508
1	Scitec Inc. ATTN: Alex Zislan 100 Wall Street Princeton, NJ 08540

Aberdeen Proving Ground

1	Dir, USAMSAA ATTN: AMXSY-D, Mr. W. Brooks Mr. R. Conroy
6	Cdr, USACSTA ATTN: STECS-TD, Mr. Kelton STECS-PO, M. Maule STECS-AS-LA, S. Walton STECS-DA, P. Paules STECS-RM-PF, S. Hinte STECS-AS-HP, J. Andrews
1	Cdr, USATECOM ATTN: AMSTE-TE-R, Mr. Keele AMSTE-TO-F
1	Dir, AMC Int. Mat. Eval. Div. ATTN: AMCICP-IM, R. Bloom
2	Dir, USAHEL ATTN: G. Garinther J. Kalb

USER EVALUATION SHEET/CHANGE OF ADDRESS

This laboratory undertakes a continuing effort to improve the quality of the reports it publishes. Your comments/answers below will aid us in our efforts.

1. Does this report satisfy a need? (Comment on purpose, related project, or other area of interest for which the report will be used.) _____

2. How, specifically, is the report being used? (Information source, design data, procedure, source of ideas, etc.) _____

3. Has the information in this report led to any quantitative savings as far as man-hours or dollars saved, operating costs avoided, or efficiencies achieved, etc? If so, please elaborate. _____

4. General Comments. What do you think should be changed to improve future reports? (Indicate changes to organization, technical content, format, etc.) _____

BRL Report Number BRL-MR-3957 Division Symbol _____

Check here if desire to be removed from distribution list. ____

Check here for address change. ____

Current address: Organization _____
Address _____

DEPARTMENT OF THE ARMY
Director
U.S. Army Ballistic Research Laboratory
ATTN: SLCBR-DD-T
Aberdeen Proving Ground, MD 21005-5066

OFFICIAL BUSINESS

BUSINESS REPLY MAIL
FIRST CLASS PERMIT No 0001, APG, MD

Postage will be paid by addressee

Director
U.S. Army Ballistic Research Laboratory
ATTN: SLCBR-DD-T
Aberdeen Proving Ground, MD 21005-5066

NO POSTAGE NECESSARY IF MAILED IN THE UNITED STATES